

# Chapter 12

## THEORY

In this Chapter the theoretical basis for WAMIT is described. Further information can be found in Reference [26], and in the references cited below.

### 12.1 THE BOUNDARY-VALUE PROBLEM

Figure 12.1 illustrates a three-dimensional body interacting with plane progressive waves in water of finite water depth  $H$ . The objective of WAMIT is to evaluate the unsteady hydrodynamic pressure, loads and motions of the body, as well as the induced pressure and velocity in the fluid domain. The free-surface and body-boundary conditions are linearized, the flow is assumed to be potential, free of separation or lifting effects. A harmonic time dependence is adopted.

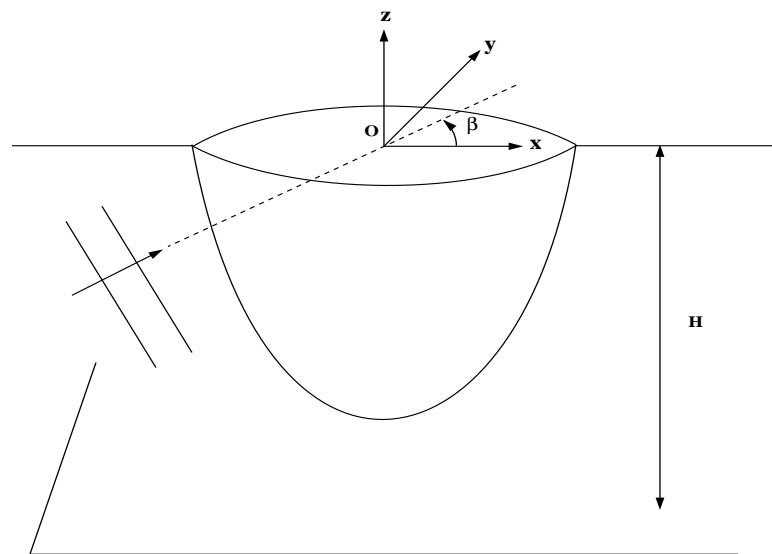


Figure 12.1: Sketch defining the coordinates, fluid depth, and wave-heading angle.

The Cartesian coordinate system  $(x, y, z)$  defined in Figure 12.1 is stationary relative to the undisturbed position of the free surface and body. Its origin may lie on, above or below the free surface as the particular application requires. The body geometry input to WAMIT is defined relative to that system. Here, the origin is located on the free surface for the sake of simplicity.

The assumption of a potential flow permits the definition of the flow velocity as the gradient of the velocity potential  $\Phi$  satisfying the Laplace equation

$$\nabla^2 \Phi = 0 \quad (12.1)$$

in the fluid domain. The harmonic time dependence allows the definition of a complex velocity potential  $\varphi$ , related to  $\Phi$  by

$$\Phi = \text{Re}(\varphi e^{i\omega t}), \quad (12.2)$$

where  $\text{Re}$  denotes the real part,  $\omega$  is the frequency of the incident wave and  $t$  is time. The ensuing boundary-value problem will be expressed in terms of the complex velocity potential  $\varphi$ , with the understanding that the product of all complex quantities with the factor  $e^{i\omega t}$  applies. The linearized form of the free-surface condition is

$$\varphi_z - K\varphi = 0, \quad z = 0 \quad (12.3)$$

where  $K = \omega^2/g$ , and  $g$  is the acceleration of gravity. The velocity potential of the incident wave is defined by

$$\varphi_0 = \frac{igA}{\omega} \frac{\cosh[\nu(z+H)]}{\cosh \nu H} e^{-i\nu x \cos \beta - i\nu y \sin \beta}, \quad (12.4)$$

where the wavenumber  $\nu$  is the real root of the dispersion relation

$$\frac{\omega^2}{g} = \nu \tanh \nu H, \quad (12.5)$$

and  $\beta$  is the angle between the direction of propagation of the incident wave and the positive  $x$ -axis as defined in Figure 12.1.

The linearization of the problem permits the decomposition of the velocity potential  $\varphi$  into the radiation and diffraction components

$$\varphi = \varphi_R + \varphi_D, \quad (12.6)$$

$$\varphi_R = i\omega \sum_{j=1}^6 \xi_j \varphi_j, \quad (12.7)$$

$$\varphi_D = \varphi_0 + \varphi_7. \quad (12.8)$$

The constants  $\xi_j$  denote the complex amplitudes of the body oscillatory motion in its six rigid-body degrees of freedom, and  $\varphi_j$  the corresponding unit-amplitude radiation potentials. The velocity potential  $\varphi_7$  represents the *scattered* disturbance of the incident wave by the body fixed at its undisturbed position. We will refer to the sum (12.8) as the *diffraction* potential  $\varphi_D$ .

On the undisturbed position of the body boundary, the radiation and diffraction potentials are subject to the conditions,

$$\varphi_{jn} = n_j, \quad (12.9)$$

$$\varphi_{Dn} = 0, \quad (12.10)$$

where  $(n_1, n_2, n_3) = \mathbf{n}$  and  $(n_4, n_5, n_6) = \mathbf{x} \times \mathbf{n}$ ,  $\mathbf{x} = (x, y, z)$ . The unit vector  $\mathbf{n}$  is normal to the body boundary and *points out of the fluid domain*.

The boundary value problem must be supplemented by a condition of outgoing waves applied to the velocity potentials  $\varphi_j$ ,  $j = 1, \dots, 7$ .

## 12.2 INTEGRAL EQUATIONS FOR THE VELOCITY POTENTIAL

In WAMIT the boundary value problems (12.1-10) are solved by using Green's theorem to derive integral equations for the radiation and diffraction velocity potentials on the body boundary. The integral equation satisfied by the radiation velocity potentials  $\varphi_j$  on the body boundary takes the form

$$2\pi\varphi_j(\mathbf{x}) + \iint_{S_b} \varphi_j(\boldsymbol{\xi}) \frac{\partial G(\boldsymbol{\xi}; \mathbf{x})}{\partial n_\xi} d\boldsymbol{\xi} = \iint_{S_b} n_j G(\boldsymbol{\xi}; \mathbf{x}) d\boldsymbol{\xi}. \quad (12.11)$$

where  $S_b$  denotes body wetted surface at calm water.

The corresponding equation for the total diffraction velocity potential  $\varphi_D$  is

$$2\pi\varphi_D(\mathbf{x}) + \iint_{S_b} \varphi_D(\boldsymbol{\xi}) \frac{\partial G(\boldsymbol{\xi}; \mathbf{x})}{\partial n_\xi} d\boldsymbol{\xi} = 4\pi\varphi_0(\mathbf{x}). \quad (12.12)$$

The diffraction potential may also be obtained from equation (12.8) after solving for the scattered potential  $\varphi_7$ . The equation for the scattered velocity potential is

$$2\pi\varphi_7(\mathbf{x}) + \iint_{S_b} \varphi_7(\boldsymbol{\xi}) \frac{\partial G(\boldsymbol{\xi}; \mathbf{x})}{\partial n_\xi} d\boldsymbol{\xi} = - \iint_{S_b} \frac{\partial \varphi_0(\boldsymbol{\xi})}{\partial n} G(\boldsymbol{\xi}; \mathbf{x}) d\boldsymbol{\xi}. \quad (12.13)$$

From the computational point of view, equation (12.12) has some advantages over equation (12.13) in terms of cpu time and the requirement of storage space, because of the relative simplicity of the right-hand side.

The Green function  $G(\mathbf{x}; \boldsymbol{\xi})$  is referred to as the wave source potential. It is the velocity potential at the point  $\mathbf{x}$  due to a point source of strength  $-4\pi$  located at the point  $\boldsymbol{\xi}$ . It satisfies the free-surface and radiation conditions, and in infinite water depth is defined by

$$G(\mathbf{x}; \boldsymbol{\xi}) = \frac{1}{r} + \frac{1}{r'} + \frac{2K}{\pi} \int_0^\infty dk \frac{e^{k(z+\zeta)}}{k-K} J_0(kR) \quad (12.14)$$

$$r^2 = (x - \xi)^2 + (y - \eta)^2 + (z - \zeta)^2 \quad (12.15)$$

$$r'^2 = (x - \xi)^2 + (y - \eta)^2 + (z + \zeta)^2, \quad (12.16)$$

where  $J_0(x)$  is the Bessel function of zero order. In finite depth, the Green function is defined by

$$G(\mathbf{x}; \boldsymbol{\xi}) = \frac{1}{r} + \frac{1}{r''} + 2 \int_0^\infty dk \frac{(k+K) \cosh k(z+H) \cosh k(\zeta+H)}{k \sinh kH - K \cosh kH} e^{-kH} J_0(kR) \quad (12.17)$$

$$(r'')^2 = (x - \xi)^2 + (y - \eta)^2 + (z + \zeta + 2H)^2. \quad (12.18)$$

In both expressions (12.14) and (12.17) the Fourier  $k$ -integration is indented above the pole on the real axis in order to enforce the radiation condition. Efficient algorithms for the evaluation of the infinite and finite-depth wave-source potentials and their spatial derivatives, have been developed in [1] and [11]. These algorithms are coded in the subroutines VGRN00 and HGRN00 which are included in WAMIT. (These subroutines supersede the earlier versions of the subroutines FGRN89, HGRN89 and IGRN89 or VGRN94, HGRN94, VGRN98 and HGRN98.)

Special attention must be given to the singular components of the Green function for small values of  $r$ ,  $r'$  and  $r''$ . The source-like singularities  $1/r$ ,  $1/r'$  and  $1/r''$  and their normal derivatives can be integrated analytically over a quadrilateral panel, as described in [2]. In addition, the ascending series expansion of the wave source potential for small values of  $r'$  (Ref. [1], eq.(5)), reveals the presence of the logarithmic singularity,

$$G(\mathbf{x}; \boldsymbol{\xi}) = \frac{1}{r} + \frac{1}{r'} - 2K \log K(r' + |z + \zeta|) + O(1), \quad (12.19)$$

(The derivation of this result in [1] is for the infinite-depth case, but it can be shown from the analysis of the finite-depth case in the same reference that the same singularity applies.) Provision has been made in WAMIT to permit the logarithmic singularity and its derivatives to be integrated analytically in the solution of the integral equations when the source and field points are close to each other and to the free surface. Further details are given in Section 12.4.

## 12.3 INTEGRAL EQUATIONS FOR THE SOURCE FORMULATION

In this Section a brief description is given of the source distribution method, which is used to derive the fluid velocity components on the body surface in the low-order method. The velocity are required to evaluate the mean second-order pressure, from which the mean drift forces and moments can be evaluated in the manner described in Section 12.7.

In source distribution method, the velocity potential is expressed by a distribution of sources only

$$\varphi(\mathbf{x}) = \iint_{S_b} \sigma(\boldsymbol{\xi}) G(\mathbf{x}; \boldsymbol{\xi}) d\boldsymbol{\xi} \quad (12.20)$$

After discretizing the body boundary with plane panels with constant source strength on each panel, the potential can be expressed by

$$\varphi(\mathbf{x}_i) = \sum_{j=1}^N \sigma(\mathbf{x}_j) \iint_{S_j} G(\mathbf{x}_i; \boldsymbol{\xi}) d\boldsymbol{\xi} \quad (12.21)$$

Denote the normal vector as  $\vec{n}$  and the two tangential unit vectors as  $\vec{s}$  and  $\vec{t}$  on each panel. The three components of the velocity are then given in the  $(\vec{n}, \vec{s}, \vec{t})$  coordinate system as follows:

$$\varphi_n(\mathbf{x}_i) = 2\pi\sigma(\mathbf{x}_i) + \sum_{j=1}^N \sigma(\mathbf{x}_j) \iint_{S_j} G_n(\mathbf{x}_i; \boldsymbol{\xi}) d\boldsymbol{\xi} \quad (12.22)$$

$$\varphi_s(\mathbf{x}_i) = \sum_{j=1}^N \sigma(\mathbf{x}_j) \iint_{S_j} G_s(\mathbf{x}_i; \boldsymbol{\xi}) d\boldsymbol{\xi} \quad (12.23)$$

$$\varphi_t(\mathbf{x}_i) = \sum_{j=1}^N \sigma(\mathbf{x}_j) \iint_{S_j} G_t(\mathbf{x}_i; \boldsymbol{\xi}) d\boldsymbol{\xi} \quad (12.24)$$

## 12.4 DISCRETIZATION OF THE INTEGRAL EQUATIONS IN THE LOW-ORDER METHOD (ILOWHI=0)

The mean position of the body wetted surface is approximated by a collection of quadrilaterals. Each quadrilateral is defined by four vertices, lying on the body surface. Their Cartesian coordinates are input to WAMIT. They are numbered in the counter-clockwise direction when the panel is viewed from the fluid domain. Instructions on how to input the vertex coordinates are given in Chapter 5.

In general the quadrilaterals defined above are not plane, but if a sufficiently fine discretization is used for a boundary surface with continuous curvature, each element will

approach a plane surface. In this circumstance a plane approximation of the general quadrilateral is defined by the midpoints of each side, which always lie in the same plane. Each *panel* is defined by projecting the four vertices onto this plane. If the coordinates of two adjacent vertices coincide, the quadrilateral panel reduces to a triangular panel.

For bodies of general shape, gaps may exist between panels. Experience suggests that they do not significantly affect the accuracy of the velocity potential and the hydrodynamic forces.

The radiation and diffraction velocity potentials are taken to be constant over each panel. The discretization errors associated with the selection of plane panels and a piecewise constant variation of the velocity potential are of the same order, if the integration of the singular components of the wave source potential over the panels are carried out with sufficient accuracy.

Based on this discretization, the continuous integral equations (12.11) and (12.12) can be reduced to a set of linear simultaneous equations for the values of the velocity potentials over the panels. For the radiation potentials we obtain

$$2\pi\varphi(\mathbf{x}_i) + \sum_{k=1}^N D_{ik}\varphi_k = \sum_{k=1}^N S_{ik} \left( \frac{\partial\varphi}{\partial n} \right)_k, \quad (12.25)$$

where  $i = 1, \dots, N$ ,  $N$  being the number of panels. For the total diffraction potential

$$2\pi\varphi(\mathbf{x}_i) + \sum_{k=1}^N D_{ik}\varphi_k = 4\pi\varphi_0(\mathbf{x}_i). \quad (12.26)$$

The matrices  $D_{ik}$  and  $S_{ik}$  are defined by

$$D_{ik} = \iint_{s_k} \frac{\partial G(\boldsymbol{\xi}, \mathbf{x}_i)}{\partial n_\xi} d\boldsymbol{\xi}, \quad (12.27)$$

$$S_{ik} = \iint_{s_k} G(\boldsymbol{\xi}, \mathbf{x}_i) d\boldsymbol{\xi}, \quad (12.28)$$

where  $s_k$  denotes the surface of the  $k$ -th panel. The ‘collocation’ points  $\mathbf{x}_i$ , where the integral equations are enforced, are located at the panel centroids.

The rest of this section describes the computation of the influence coefficients  $D_{ik}$  and  $S_{ik}$ .

If the index IDIAG=0 in the potential control file (see Section 3.1), the characteristic length scale DIAG(2) for a given panel is equal to the square root of its area; if IDIAG=1, DIAG(2) is equal to the length of the largest diagonal of the panel. The setting of the index IDIAG applies to all the panels. The selection IDIAG=1 is more conservative, and results in an increase in the number of pairs of panels for which the Rankine singularities are integrated analytically. The Rankine and logarithmic singularities of the wave source potential are subtracted and integrated analytically over the panels if the distance between the centroids of the  $i$ -th and  $j$ -th panels is less than  $10 \times \text{DIAG}(2)$ . This comparison is

based on the maximum  $\text{DIAG}(2)$  of the pair of panels. Assuming that the collocation point is located on the  $i$ -th panel, it is reflected about the free surface and the bottom (if present). The distance of its reflections from the centroid of the  $j$ -th panel are denoted by  $r'$  (above the free surface) and  $r''$  (below the bottom). The integrals of the  $1/r'$  and  $1/r''$  singularities are evaluated as for the  $1/r$  singularity, using analytic integration over the  $j$ -th panel, when these distances are less than  $10 \times \text{DIAG}(2)$ . When the index  $\text{ILOG}=1$  the logarithmic singularity is subtracted and integrated analytically along with  $1/r'$ . When any of the Rankine and logarithmic singularities is not subtracted and integrated analytically, it is incorporated in the evaluation of the wave source potential by `VGRN00`.

The index  $\text{ILOG}$ , also set in the potential control file, controls the analytical integration of the logarithmic singularity. When  $\text{ILOG}=1$ , the logarithmic singularity is subtracted and integrated analytically for the same pairs of panels for which the Rankine singularity  $1/r'$  is integrated analytically. When  $\text{ILOG}=0$  the singularity is included in the evaluation of the wave-source potential and integrated by quadrature.

The integrals of the  $1/r$ ,  $1/r'$ ,  $\log[r' - (z + \zeta)]$  and  $1/r''$  singularities over the panels are frequency independent and are carried out once for all frequencies for the relevant pairs of panels. These integrals are stored in a file for use at each frequency. The evaluation of the Rankine integrals is accompanied by the set-up of an integer array of indices to indicate which singularities have been subtracted for each pair of panels. These indices are input to `VGRN00`, which in turn evaluates the appropriate component of the wave source potential.

The analytic integration of the Rankine source potentials and their derivatives follows the theory outlined in [2]. Depending on the radial distance to the field point, relative to the panel length-scale  $\text{DIAG}(2)$ , the evaluations are performed either from the exact formulation or from multipole expansions including either second- or fourth-moments of the panel area. The radial distances for transitions between these three algorithms are based on the requirement of six-decimal relative accuracy. The formulae used for the analytic integration of the logarithmic singularity are derived in [6].

The integration over each panel of the regular part of the wave source potential (evaluated in `VGRN00`) is carried out by quadrature. Two alternative quadrature formulae are used in `WAMIT`, depending on the input parameter `IQUAD`. If `IQUAD=0` the centroid integration formula is used, where the integral over each panel is approximated by multiplying the value of the integrand at the centroid by the panel area. If `IQUAD=1` the Gauss integration formula is used with four nodes and corresponding weights over each panel, by mapping their surface to a unit square using a bilinear transformation. The wave source potential can be integrated over the panels by either method. When the centroid integration is selected, `WAMIT` exploits the symmetry of the wave source potential with respect to the position of the source and field points to evaluate the wave source potential once for each pair of panels. Thus, if there are  $N$  panels and no planes of symmetry,  $N^2/2$  calls are made to `VGRN00`. The selection of the four-node Gauss quadrature formula requires  $4N^2$  calls to `VGRN00` since the wave source potential symmetries cannot be utilized. For a sufficiently large number of panels, the use of the centroid integration has been found to be sufficiently accurate, and is recommended.

## 12.5 DISCRETIZATION OF THE INTEGRAL EQUATIONS IN THE HIGHER-ORDER METHOD (ILOWHI=1)

The mean body surface is defined by ‘patches’, as explained in Chapter 6. Each patch must be a smooth continuous surface. The Cartesian coordinates  $\mathbf{x} = (x, y, z)$  of a point on the patch are expressed in term of two parametric coordinates  $\mathbf{u} = (u, v)$ . The latter is normalized so that they vary in  $\pm 1$ . Details of geometric description of the body surface are provided in Section 6.1.

The velocity potential on each patch is represented by a product of B-spline basis functions  $U(u)$  and  $V(v)$  as shown in equation (6.4). The total number of B-spline basis functions on each patch is  $M_u$  times  $M_v$ .

Upon substituting equations (6.3) and (6.4), (12.11) can be expressed in a form

$$\begin{aligned} 2\pi \sum_{m=1}^{M_v} \sum_{l=1}^{M_u} (\phi_j)_k \mathbf{U}_k(\mathbf{u}_f) &+ \sum_{n=1}^{N_p} \iint d\mathbf{u} \sum_{m=1}^{M_v} \sum_{l=1}^{M_u} (\phi_j)_k \mathbf{U}_k(\mathbf{u}) \frac{\partial G(\mathbf{u}; \mathbf{u}_f)}{\partial n(\mathbf{u})} J(\mathbf{u}) \\ &= \sum_{n=1}^{N_p} \iint d\mathbf{u} \frac{\partial \phi_j}{\partial n}(\mathbf{u}) G(\mathbf{u}; \mathbf{u}_f) J(\mathbf{u}) \end{aligned} \quad (12.29)$$

where,  $\mathbf{U}_k = U_l(u)V_m(v)$ ,  $\iint d\mathbf{u} = \int_{-1}^1 dv \int_{-1}^1 du$ ,  $J(\mathbf{u})$  is Jacobian and  $N_p$  denotes the number of patches.

Following the Galerkin method, (12.29) is multiplied by  $\mathbf{U}_i$  and integrated over each patch. This results in the linear system

$$2\pi d_{ik}^H(\phi_j)_k + \sum_{k=1}^N D_{ik}^H(\phi_j)_k = S_i^H \quad (12.30)$$

for the radiation potential. Similarly, from (12.12), we obtain

$$2\pi d_{ik}^H(\phi_D)_k + \sum_{k=1}^N D_{ik}^H(\phi_D)_k = I_i^H \quad (12.31)$$

for the diffraction potential.

In the above equations,  $(\phi_j)_k$  and  $(\phi_D)_k$  are unknown coefficients of basis function for the radiation and diffraction potentials, respectively. The matrices  $d_{ik}^H$  and  $D_{ik}^H$  and vectors  $S_i^H$  and  $I_i^H$  are defined by

$$d_{ik}^H = \iint d\mathbf{u}_f \mathbf{U}_i(\mathbf{u}_f) \mathbf{U}_k(\mathbf{u}_f) \quad (12.32)$$

$$D_{ik}^H = \iint d\mathbf{u}_f \mathbf{U}_i(\mathbf{u}_f) \iint d\mathbf{u} \mathbf{U}_k(\mathbf{u}) \frac{\partial G(\mathbf{u}; \mathbf{u}_f)}{\partial n(\mathbf{u})} J(\mathbf{u}) \quad (12.33)$$

$$S_i^H = \iint d\mathbf{u}_f \mathbf{U}_i(\mathbf{u}_f) \iint d\mathbf{u} \frac{\partial \phi_j}{\partial n}(\mathbf{u}) G(\mathbf{u}; \mathbf{u}_f) J(\mathbf{u}) \quad (12.34)$$

$$I_i^H = \iint d\mathbf{u}_f \mathbf{U}_i(\mathbf{u}_f) \varphi_0(\mathbf{u}_f) \quad (12.35)$$

As explained in Chapter 6, a set of B-spline basis functions is defined by the order of the polynomial ( $K_u$  and  $K_v$ ) and the number of panels ( $N_u$  and  $N_v$ ). In general, the basis function has nonzero value over a part of the patch. For example,  $U_l(u)V_m(v)$  is nonzero on the panels from  $l - K_u + 1$ - (or 1, if  $l - K_u + 1 < 1$ ) to  $l$ -th panels (or  $N_u$ , if  $l > N_u$ ) in  $u$  and  $m - K_v + 1$ - (or 1, if  $m - K_v + 1 < 1$ ) to  $m$ -th (or  $N_v$ , if  $m > N_v$ ) panels in  $v$ .

The integration in  $\mathbf{u}_f$  over each panel is referred to as the ‘outer’ integration. This is carried out by Gauss-Legendre quadrature. The order of the quadrature is specified by the input parameters IQUO and IQVO in the SPL file, for  $u$  and  $v$  respectively, or by the parameter IQUADO in CONFIG.WAM. The order of the basis functions are specified by the parameters KU and KV in the SPL file, or KSPLIN in CONFIG.WAM.

The *inner* integrations in  $\mathbf{u}$  in equations (12.33) and (12.34) are carried out as described below, for each abscissa of the Gaussian quadrature for the outer integral,  $\mathbf{u}_f$ .

The integration of the regular part of the wave source potential (evaluated in VGRN00) is carried out by Gauss-Legendre quadrature. The order of the inner quadrature is specified by the input parameters IQUI and IQVI in the SPL file or by the parameter IQUADI in CONFIG.WAM. Numerical tests suggest that the order of the quadrature should be one order higher than the order of the basis function.

The integrals involving the Rankine source and normal dipole are evaluated in the manner explained next. If the field point  $\mathbf{u}_f$  is on the panel, the integrand is singular at this point. Otherwise the integrand is regular throughout the domain of the panel. In the singular case, the panel is subdivided into a small square subdomain centered at the field point  $\mathbf{u}_f$ , and one or more rectangular subdivisions adjoining the square as required to cover the remainder of the panel. The integrals over the latter subdivisions are treated in the same manner as for the other panels where the integrand is regular.

The integrals where the integrand is regular are evaluated by Gauss-Legendre quadrature. If the field point is near the panel, the panel is subdivided into four smaller panels. This subdivision is repeated until the size of the subdivided panel is less than a prescribed multiple of the physical distance from  $\mathbf{u}_f$  to the centroid of the panel. For this purpose the size of the panel is defined as the maximum physical length from the center of the panel to its four vertices. The maximum size permitted without further subdivision is  $1/\sqrt{2.25} = 2/3$ . In some cases a large number of subdivisions are required, particularly when  $\mathbf{u}_f$  is close to the sides or vertices of the panel. In this case, the program terminates subdivision after the domain is subdivided into 2048 subdomains. The program issues a warning message to the monitor and error log file but continues without interruption. Experience indicates that this warning message is most likely to occur when the mapping of a physical surface onto a patch is singular, as at the poles of a spherical or spheroidal surface, and that the accuracy of most relevant hydrodynamic outputs are not affected significantly by this problem.

The singular integral over the square subdomain centered at  $\mathbf{u}_f$  is explained below. The integration of the dipole is defined in the ‘principal-value’ sense excluding a vanishingly small area around the origin. With this definition for the dipole integral, both the source

and dipole distributions can be evaluated in a same manner.

After an appropriate normalization of the length and use of a local coordinates with the origin at  $(u_f, v_f)$ , the integral takes a form

$$I = \int_{-1}^1 \int_{-1}^1 \frac{A(u, v)}{|\mathbf{x}(u, v)|} dudv \quad (12.36)$$

where  $A(u, v)$  is regular function.  $|\mathbf{x}(u, v)|$  is the distance between the source and field points in physical space.

For simplicity, we consider only a case where  $|\frac{\partial \mathbf{x}}{\partial u}| = 1$ ,  $|\frac{\partial \mathbf{x}}{\partial v}| = 1$  and  $\frac{\partial \mathbf{x}}{\partial u} \cdot \frac{\partial \mathbf{x}}{\partial v} = 0$  but the analysis below can be applied directly to the general case. Since  $|\mathbf{x}|/\sqrt{u^2 + v^2}$  is regular and thus (12.36) can be expressed in the form

$$I = \int_{-1}^1 \int_{-1}^1 \frac{f(u, v)}{\sqrt{u^2 + v^2}} dudv \quad (12.37)$$

where  $f(u, v)$  is regular.

The singularity at the origin is removed by subdividing the square domain into 4 isosceles triangles with a common vertex at the origin and evaluating the integral separately over each triangle. For example, the integral over a triangle with a side on  $u = 1$  is

$$I^{(1)} = \int_0^1 du \int_{-u}^u dv \frac{f(u, v)}{\sqrt{u^2 + v^2}} \quad (12.38)$$

After the change of variables  $u = p$ ,  $v = pq$ , we have

$$I^{(1)} = \int_0^1 dp \int_{-1}^1 dq \frac{f(p, pq)}{\sqrt{1 + q^2}} \quad (12.39)$$

After adding the contributions from other three triangles, we have

$$I = \int_{-1}^1 dp \int_{-1}^1 dq \frac{f(p, pq) + f(pq, p)}{\sqrt{1 + q^2}} \quad (12.40)$$

Next we remove the square root function from (12.40). By change of the variables  $q = \sinh(as)$ , we have

$$I = a \int_{-1}^1 dp \int_{-1}^1 ds f(p, p \sinh as) + f(p \sinh as, p) \quad (12.41)$$

where  $a = \sinh^{-1}1$ . The integral (12.41) is evaluated by applying the Gauss-Legendre quadrature in  $p$  and  $s$  coordinates.

The integral of the log singularity in the free-surface component of the source potential can be evaluated either in a similar manner as for the Rankine source, or together with the regular part of the wave source potential. The index ILOG, set in the potential control file or in CONFIG.WAM controls these options. When ILOG=1, the logarithmic singularity is subtracted from the wave-source potential and integrated separately. When ILOG=0 it is included in the evaluation of the wave-source potential and integrated by the same quadrature.

## 12.6 SOLUTION OF THE LINEAR SYSTEMS

The procedure used to solve the linear systems (12.25-6) or (12.30-1) is essentially the same. The dimension of these linear systems is denoted by NEQN (number of equations). In the low-order method NEQN is the same as the number of panels. In the higher-order method NEQN depends on the number of patches, panels, and on the order of the basis functions, as explained in Section 12.5.

If the body geometry has one or two planes of symmetry, half or a quarter of its wetted surface is represented with panels, respectively. Each of the radiation potentials is symmetric or anti-symmetric with respect to the symmetry planes, depending on the rigid-body mode, and the diffraction potential is decomposed into similar components. Thus for one or two planes of symmetry either two or four separate components of the diffraction problem are defined on the basis of their symmetry or anti-symmetry with respect to the  $x$ - and  $y$ -planes. With this decomposition the dimensions of all linear systems are the same as NEQN.

Flow symmetries and anti-symmetries are enforced in the solution of the integral equations by the method of images. The collocation point  $\mathbf{x}_i$  in the argument of the wave source potential, is reflected about the geometry symmetry planes accompanied by a multiplication by  $+1$  or  $-1$  for symmetric and antisymmetric flow, respectively.

To avoid unnecessary computations, the architecture of WAMIT permits the analysis of any desired sub-set of the rigid-body modes and of the corresponding diffraction components, based on the settings of the MODE(I) indices in the potential control file (see Section 3.1). For example, if only the heave mode is specified in conjunction with the solution of the diffraction problem, and if there are planes of symmetry, only the symmetric component of the diffraction potential is evaluated. For this reason it is necessary to specify the complete diffraction solution (IDIFF= 1) to evaluate field data (free surface elevation, pressure, and fluid velocity) or to evaluate the drift forces.

With the default value of the input parameter ISOLVE=0, WAMIT solves the linear systems in the radiation and diffraction problems by means of a special out-of-core iterative solver. The maximum number of iterations is controlled by the parameter MAXITT in the config.wam file (Section 3.7), with the default value equal to 35. When convergence is not achieved within the limit, a warning message is printed to the on monitor, and the computation continues without interruption. If the number of iterations displayed in the output is equal to MAXITT, this also indicates that convergence does not occur.

A supplementary direct solver for the linear systems may be used for the case for which the iterative solver is nonconverging or slowly converging. It is based on standard Gauss reduction, with partial pivoting. The LUD algorithm is employed for efficiency in solving several linear systems simultaneously, with different right-hand sides. The direct solver also can be used to confirm the iterative solution, and in cases where the number of equations (NEQN) is relatively small the direct solver can result in reduced computing time, particularly if the number of right-hand sides is large.

WAMIT also includes a block-iterative solver to provide increased options in the solution of the linear system. This solver is based on the same algorithm as the iterative solver,

but the local LU decompositions are performed for specified blocks adjacent to the main diagonal. At each iteration the back substitution is performed for each block, at each stage of iterations. This accelerates the rate of convergence, and as the dimension of the blocks increases the limiting case is the same as the direct solver. The opposite limit is the case when the dimension of the blocks is one, which is the result of setting ISOLVE=NEQN; in this case the result is identical to using the iterative solver without blocks (ISOLVE=0).

The convergence of the iterative method is quite different for the low- and higher-order methods. The primary reason for the slow convergence of the higher-order method is that the linear system loses diagonal dominance as the order of basis function increases as shown in the expression for  $d_{ik}^H$  in (12.32).

Usually in the low-order method the number of iterations required to obtain convergence is in the range 10-20, and the iterative solver is most effective. In the higher-order method experience indicates that the convergence rate is reduced, and it is generally advisable to use the direct solver (ISOLVE= 1) or, in cases where NEQN is very large, the block-iterative solver (ISOLVE> 1). For special problems where hydrodynamic resonances occur, the convergence rate is reduced and it is necessary to use the direct or block-iterative solver also with the low-order method.

Experience using the low-order method has shown that slow convergence is infrequent, and limited generally to special applications where there either is a hydrodynamic resonance in the fluid domain, as in the gap between two adjacent barges, or in the non-physical domain exterior to the fluid volume. An example of the latter is a barge of very shallow draft, where the irregular frequencies are associated with non-physical modes of resonant wave motion inside the barge. These types of problems can often be overcome by modifying the arrangement of the panels or increasing the number of panels.

For the low-order method various convergence tests have been published in References 5, 6, 9, 10 and 12, based on applications of WAMIT. The accuracy of the evaluated quantities has been found to increase with increasing numbers of panels, thus ensuring the convergence of the discretization scheme. The condition number of the linear systems is relatively insensitive to the order of the linear systems, and sufficiently small to permit the use of single-precision arithmetic. Convergence tests for the higher-order method are reported in References 18, 19, 20, 24 and 25.

## 12.7 MEAN DRIFT FORCE AND MOMENT BASED ON PRESSURE INTEGRATION

The instantaneous position vector ( $\vec{X}$ ) in an inertial coordinate system of the point fixed on the body fixed coordinate system ( $\vec{x}$ ) is given by

$$\vec{X} = \vec{x} + \vec{\xi} + \vec{\alpha} \times \vec{x} + H\vec{x} \quad (12.42)$$

For the present purpose we consider only the first order quantities of the translational modes  $\vec{\xi}$ , the rotational modes  $\vec{\alpha}$  and the velocity potential  $\phi$ . The roll-pitch-yaw sequence of rotations is adopted, and the transformation matrix is given by

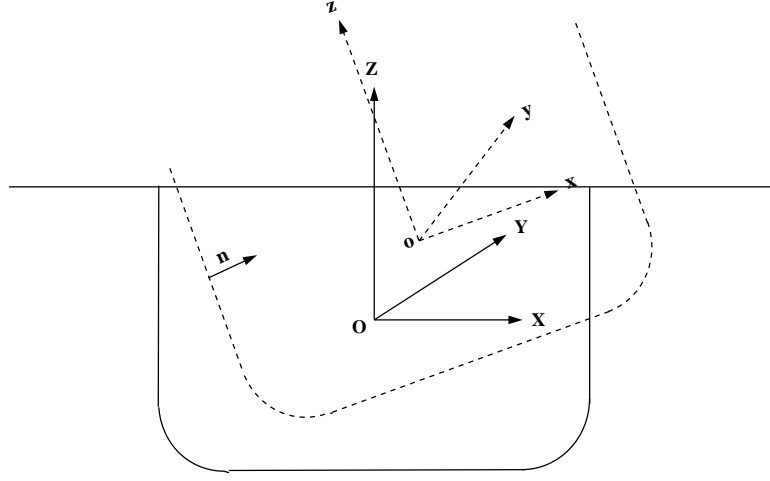


Figure 12.2: Coordinate systems fixed with respect to the body (dashed lines) and its mean position (solid lines)

$$H = \frac{1}{2} \begin{pmatrix} -(\alpha_2^2 + \alpha_3^2) & 0 & 0 \\ 2\alpha_1\alpha_2 & -(\alpha_1^2 + \alpha_3^2) & 0 \\ 2\alpha_1\alpha_3 & 2\alpha_2\alpha_3 & -(\alpha_1^2 + \alpha_2^2) \end{pmatrix} \quad (12.43)$$

The normal vector in the inertial coordinate system can be expressed by

$$\vec{N} = \vec{n} + \vec{\alpha} \times \vec{n} + H\vec{n} \quad (12.44)$$

where  $\vec{n}$  is the normal vector on the body boundary in the body fixed coordinate system.

The pressure at the instantaneous position  $\vec{X}$  given in the equation (12.42) can be expressed by

$$P = -\rho[g(z + Z_o) + (\phi_t + g(\xi_3 + \alpha_1 y - \alpha_2 x)) + (\frac{1}{2}\nabla\phi \cdot \nabla\phi + (\vec{\xi} + \vec{\alpha} \times \vec{x}) \cdot \nabla\phi_t + gH\vec{x} \cdot \nabla z)] \quad (12.45)$$

where  $Z_o$  is the vertical coordinate of  $O$  relative to the free-surface.

The mean forces and moments are obtained by time averaging the following expressions for the forces and moments:

$$\vec{F}^{(2)} = \iint_{\tilde{S}_b} \vec{N} P ds \quad (12.46)$$

$$\vec{M}^{(2)} = \iint_{\tilde{S}_b} (\vec{X} \times \vec{N}) P ds \quad (12.47)$$

In equations (12.46) and (12.47), the integrations are over the exact body wetted surface  $\tilde{S}_b$ .

After substituting (12.42), (12.44), and (12.45) and integrating the hydrostatic components,

$$\begin{aligned}
\vec{F}^{(2)} &= \frac{1}{2}\rho g \int_{WL} \vec{n}'[\zeta^2 - 2\zeta(\xi_3 + \alpha_1 y - \alpha_2 x)]dl \\
&+ \frac{1}{2}\rho g \vec{k} \int_{WL} \frac{n_z}{\sqrt{1-n_z^2}}[\zeta - (\xi_3 + \alpha_1 y - \alpha_2 x)]^2 dl \\
&- \rho \iint_{S_b} \vec{n} \left( \frac{1}{2} \nabla \phi \cdot \nabla \phi + (\vec{\xi} + \vec{\alpha} \times \vec{x}) \cdot \nabla \phi_t \right) ds \\
&+ \vec{\alpha} \times (-\rho \iint_{S_b} \vec{n} \phi_t ds) \\
&+ \vec{F}_S^{(2)}
\end{aligned} \tag{12.48}$$

where  $\vec{F}_S^{(2)} = -\rho g A_{wp} [\alpha_1 \alpha_3 x_f + \alpha_2 \alpha_3 y_f + \frac{1}{2}(\alpha_1^2 + \alpha_2^2) Z_o] \vec{k}$

$$\begin{aligned}
\vec{M}^{(2)} &= \frac{1}{2}\rho g \int_{WL} (\vec{x} \times \vec{n}')[\zeta^2 - 2\zeta(\xi_3 + \alpha_1 y - \alpha_2 x)]dl \\
&+ \frac{1}{2}\rho g \int_{WL} \frac{n_z}{\sqrt{1-n_z^2}} (\vec{x} \times \vec{k})[\zeta - (\xi_3 + \alpha_1 y - \alpha_2 x)]^2 dl \\
&- \rho \iint_{S_b} (\vec{x} \times \vec{n}) \left( \frac{1}{2} \nabla \phi \cdot \nabla \phi + (\vec{\xi} + \vec{\alpha} \times \vec{x}) \cdot \nabla \phi_t \right) ds \\
&- \rho \vec{\alpha} \times \iint_{S_b} (\vec{x} \times \vec{n}) \phi_t ds \\
&+ \vec{\xi} \times (-\rho \iint_{S_b} \vec{n} \phi_t ds) \\
&+ \vec{M}_S^{(2)}
\end{aligned} \tag{12.49}$$

$$\begin{aligned}
\vec{M}_S^{(2)} &= \rho g \{ \quad [ \quad (\xi_2 \alpha_2 - \xi_3 \alpha_3) A_{wp} x_f - \xi_2 \alpha_1 A_{wp} y_f \\
&\quad + \alpha_1 \alpha_2 A_{wp} x_f Z_o - \left( \frac{3}{2} \alpha_1^2 + \frac{1}{2} \alpha_2^2 \right) A_{wp} y_f Z_o \\
&\quad - \xi_2 \xi_3 A_{wp} - \xi_3 \alpha_1 A_{wp} Z_o \\
&\quad + \alpha_2 \alpha_3 (L_{11} - L_{22}) - 2\alpha_1 \alpha_3 L_{12} \\
&\quad + \alpha_1 \alpha_2 \forall x_b - \frac{1}{2} (\alpha_1^2 + \alpha_3^2) \forall y_b ] \vec{i} \\
&\quad [ \quad -\xi_1 \alpha_2 A_{wp} x_f + (\xi_1 \alpha_1 - \xi_3 \alpha_3) A_{wp} y_f \\
&\quad + \left( \frac{1}{2} \alpha_1^2 + \frac{3}{2} \alpha_2^2 \right) A_{wp} x_f Z_o - \alpha_1 \alpha_2 A_{wp} y_f Z_o \\
&\quad + \xi_1 \xi_3 A_{wp} - \xi_3 \alpha_2 A_{wp} Z_o \\
&\quad + \alpha_1 \alpha_3 (L_{11} - L_{22}) + 2\alpha_2 \alpha_3 L_{12}
\end{aligned}$$

$$+ \frac{1}{2}(\alpha_2^2 + \alpha_3^2)\forall x_b \vec{j}\} \quad (12.50)$$

$\zeta$  is the first order runup,  $A_{wp}$  is the waterplane area and  $\forall$  is the volume of the body. In addition  $(x_f, y_f)$  are the coordinates of the center of flotation,  $(x_b, y_b, z_b)$  are the coordinates of the center of buoyancy,  $(\vec{i}, \vec{j}, \vec{k})$  are positive unit vectors relative to the  $x, y, z$  coordinates, and  $L_{ij} = \int_{wp} x_i x_j ds$  denotes the moments of the waterplane area.

## 12.8 REMOVAL OF IRREGULAR FREQUENCIES

The irregular frequency effects are removed from the velocity potential and the source strength using the extended boundary integral equations. The details of discussion on the method are provided in Reference [8] and [16].

The extended boundary integral equation for the potential formulation (12.11) takes a form

$$\begin{aligned} 2\pi\varphi(\mathbf{x}) + \iint_{S_b} \varphi(\boldsymbol{\xi}) \frac{\partial G(\mathbf{x}; \boldsymbol{\xi})}{\partial n_\xi} d\boldsymbol{\xi} + \iint_{S_i} \varphi'(\boldsymbol{\xi}) \frac{\partial G(\mathbf{x}; \boldsymbol{\xi})}{\partial n_\xi} d\boldsymbol{\xi} \\ = \iint_{S_b} \frac{\partial \varphi(\boldsymbol{\xi})}{\partial n_\xi} G(\mathbf{x}; \boldsymbol{\xi}) d\boldsymbol{\xi} \quad \mathbf{x} \in S_b \end{aligned} \quad (12.51)$$

$$\begin{aligned} -4\pi\varphi'(\mathbf{x}) + \iint_{S_b} \varphi(\boldsymbol{\xi}) \frac{\partial G(\mathbf{x}; \boldsymbol{\xi})}{\partial n_\xi} d\boldsymbol{\xi} + \iint_{S_i} \varphi'(\boldsymbol{\xi}) \frac{\partial G(\mathbf{x}; \boldsymbol{\xi})}{\partial n_\xi} d\boldsymbol{\xi} \\ = \iint_{S_b} \frac{\partial \varphi(\boldsymbol{\xi})}{\partial n_\xi} G(\mathbf{x}; \boldsymbol{\xi}) d\boldsymbol{\xi} \quad \mathbf{x} \in S_i \end{aligned} \quad (12.52)$$

Here  $\varphi(\mathbf{x})$  is the unknown velocity potential on the body surface  $S_b$  and  $\varphi'(\mathbf{x})$  is the nonphysical velocity potential on the interior free surface  $S_i$ .

The corresponding equation for the source formulation (12.22) takes a form

$$2\pi\sigma(\mathbf{x}) + \iint_{S_b} \sigma(\boldsymbol{\xi}) \frac{\partial G(\mathbf{x}; \boldsymbol{\xi})}{\partial n_x} d\boldsymbol{\xi} + \iint_{S_i} \sigma(\boldsymbol{\xi}) \frac{\partial G(\mathbf{x}; \boldsymbol{\xi})}{\partial n_x} d\boldsymbol{\xi} = \frac{\partial \varphi(\boldsymbol{\xi})}{\partial n_x} \quad \mathbf{x} \in S_b \quad (12.53)$$

$$-4\pi\sigma(\mathbf{x}) + \iint_{S_b} \sigma(\boldsymbol{\xi}) \frac{\partial G(\mathbf{x}; \boldsymbol{\xi})}{\partial n_x} d\boldsymbol{\xi} + \iint_{S_i} \sigma(\boldsymbol{\xi}) \frac{\partial G(\mathbf{x}; \boldsymbol{\xi})}{\partial n_x} d\boldsymbol{\xi} = \frac{\partial \varphi(\boldsymbol{\xi})}{\partial n_x} \quad \mathbf{x} \in S_i \quad (12.54)$$

## 12.9 INTEGRAL EQUATION FOR BODIES WITH THIN SUBMERGED ELEMENTS

Green's integral equations in Section 12.2 become singular as the thickness of the body (or part of the body) decreases. To avoid this singularity in the discretized problem, the panel size should be of the same order as the thickness, or smaller, in order to render the linear system well-conditioned. Thus the size of the linear system becomes large as the thickness decreases.

An alternative form, which is nonsingular, can be obtained from Green's integral equation for the limit when the thickness is zero. In this modified form of the integral equation, the velocity potential is represented by a distribution of dipoles only, without sources. The dipole strength is equal to the difference of the velocity potential on two opposite sides of the zero-thickness surface, denoted by  $\Delta\phi$  below.

If the body surface  $S_b$  consists partly of thin 'dipole' elements  $S_d$  and partly of conventional 'source' elements  $S_s$  which are represented by both sources and dipoles, Green's integral equations (12.11-13) and the dipole distribution can be combined in the following form:

$$2\pi\phi(\mathbf{x}) + \iint_{S_s} \phi G_{n_\xi} dS_\xi + \iint_{S_d} \Delta\phi G_{n_\xi} dS_\xi = \iint_{S_s} \phi_{n_\xi} G dS_\xi \quad (12.55)$$

when  $\mathbf{x}$  is on the conventional body surface  $S_s$  and

$$\iint_{S_s} \phi G_{n_\xi n_x} dS_\xi + \iint_{S_d} \Delta\phi G_{n_\xi n_x} dS_\xi = -4\pi\phi_{n_x} + \iint_{S_s} \phi_{n_\xi} G_{n_x} dS_\xi \quad (12.56)$$

when  $\mathbf{x}$  is on the surface of zero thickness  $S_d$ .

Instructions for using this option are in Sections 5.4 and 6.10. TEST09 and TEST21, described in Appendix A, are examples of its use.

- It should be emphasized that thin dipole elements must be submerged, in contact with the fluid on both sides. A thin element which is in the plane of the free surface, and only in contact with the fluid on the lower side, should be considered as part of the conventional surface  $S_s$ .

## 12.10 MEAN DRIFT FORCE AND MOMENT USING CONTROL SURFACE

The mean drift force and moment are evaluated by one the following two alternatives depending on the value of ICTRSURF in the CFG file.

Alternative 1:

$$\vec{F}^{(2)} = - \frac{1}{2}\rho g \int_{CL} \vec{n}' \zeta^2 dl - \rho g \vec{k} \int_{WL} \zeta [(\vec{\xi} + \vec{\alpha} \times \vec{x}) \cdot \vec{n}'] dl$$

$$\begin{aligned}
& + \frac{1}{2}\rho g \vec{k} \int_{WL} \frac{n_z}{\sqrt{1-n_z^2}} [\zeta - (\xi_3 + \alpha_1 y - \alpha_2 x)]^2 dl \\
& - \rho \iint_{S_c} [\nabla \phi \frac{\partial \phi}{\partial n} - \frac{1}{2} \vec{n} (\nabla \phi \cdot \nabla \phi)] ds \\
& + \rho \vec{k} \iint_{S_f} (\zeta \frac{\partial \phi_t}{\partial z} + \frac{1}{2} \nabla \phi \cdot \nabla \phi) ds + \vec{F}_S^{(2)}
\end{aligned} \tag{12.57}$$

$$\begin{aligned}
\vec{M}^{(2)} = & - \frac{1}{2}\rho g \int_{CL} (\vec{x} \times \vec{n}') \zeta^2 dl - \rho g \int_{WL} \zeta [(\vec{\xi} + \vec{\alpha} \times \vec{x}) \cdot \vec{n}'] (\vec{x} \times \vec{k}) dl \\
& + \frac{1}{2}\rho g \int_{WL} \frac{n_z}{\sqrt{1-n_z^2}} (\vec{x} \times \vec{k}) [\zeta - (\xi_3 + \alpha_1 y - \alpha_2 x)]^2 dl \\
& - \rho \iint_{S_c} [(\vec{x} \times \nabla \phi) \frac{\partial \phi}{\partial n} - \frac{1}{2} (\vec{x} \times \vec{n}) (\nabla \phi \cdot \nabla \phi)] ds \\
& + \rho \iint_{S_f} (\vec{x} \times \vec{k}) (\zeta \frac{\partial \phi_t}{\partial z} + \frac{1}{2} \nabla \phi \cdot \nabla \phi) ds + \vec{M}_S^{(2)}
\end{aligned} \tag{12.58}$$

Alternative 2:

$$\begin{aligned}
\vec{F}^{(2)} = & \frac{1}{2}\rho g \int_{WL} \vec{n}' \zeta^2 dl - \rho g \iint_{S_f} \zeta \nabla' \zeta ds \\
& - \rho g \vec{k} \int_{WL} \zeta [(\vec{\xi} + \vec{\alpha} \times \vec{x}) \cdot \vec{n}'] dl \\
& + \frac{1}{2}\rho g \vec{k} \int_{WL} \frac{n_z}{\sqrt{1-n_z^2}} [\zeta - (\xi_3 + \alpha_1 y - \alpha_2 x)]^2 dl \\
& - \rho \iint_{S_c} [\nabla \phi \frac{\partial \phi}{\partial n} - \frac{1}{2} \vec{n} (\nabla \phi \cdot \nabla \phi)] ds \\
& + \rho \vec{k} \iint_{S_f} (\zeta \frac{\partial \phi_t}{\partial z} + \frac{1}{2} \nabla \phi \cdot \nabla \phi) ds + \vec{F}_S^{(2)}
\end{aligned} \tag{12.59}$$

$$\begin{aligned}
\vec{M}^{(2)} = & \frac{1}{2}\rho g \int_{WL} (\vec{x} \times \vec{n}') \zeta^2 dl - \rho g \iint_{S_f} \zeta (\vec{x} \times \nabla' \zeta) ds \\
& - \rho g \int_{WL} \zeta [(\vec{\xi} + \vec{\alpha} \times \vec{x}) \cdot \vec{n}'] (\vec{x} \times \vec{k}) dl \\
& + \frac{1}{2}\rho g \int_{WL} \frac{n_z}{\sqrt{1-n_z^2}} (\vec{x} \times \vec{k}) [\zeta - (\xi_3 + \alpha_1 y - \alpha_2 x)]^2 dl \\
& - \rho \iint_{S_c} [(\vec{x} \times \nabla \phi) \frac{\partial \phi}{\partial n} - \frac{1}{2} (\vec{x} \times \vec{n}) (\nabla \phi \cdot \nabla \phi)] ds \\
& + \rho \iint_{S_f} (\vec{x} \times \vec{k}) (\zeta \frac{\partial \phi_t}{\partial z} + \frac{1}{2} \nabla \phi \cdot \nabla \phi) ds + \vec{M}_S^{(2)}
\end{aligned} \tag{12.60}$$

In these equations  $S_c$  is the submerged part of the control surface,  $S_f$  is the part of the control surface on the free surface,  $WL$  is the body waterline and  $CL$  is the common boundary of  $S_c$  and  $S_f$ .  $\vec{n}'$  denotes the two-dimensional normal vector in the horizontal plane on the body waterline, pointing into the body,  $\nabla'$  is the gradient in the horizontal plane, and  $\vec{k}$  is the unit vector pointing vertically upward.  $\vec{F}_S^{(2)}$  and  $\vec{M}_S^{(2)}$  are the same as those in the equation (12.48) and (12.49). The derivations of the equations (12.57-12.60) from (12.48-12.49) are given in Reference [28].

## 12.11 INTERNAL TANK EFFECTS

The solution for the velocity potential in each tank, and the resulting forces and moments, are computed in a similar manner as for the exterior domain outside the body or bodies. Since there is no diffraction potential to consider, the velocity potential  $\phi$  in each tank is

$$\phi = i\omega \sum \xi_j \phi_j \quad (12.61)$$

and the first-order pressure at a fixed point on the tank surface is given by

$$P = -\rho g(z - Z_T + \xi_3 + \alpha_1 y - \alpha_2 x) - \rho \phi_t \quad (12.62)$$

Here  $Z_T$  is the vertical coordinate of the tank free surface above the origin.

The solution for the velocity potential  $\phi$  in each tank is computed simultaneously with the potential in the exterior fluid domain outside the hull, using one extended linear system which includes all of the fluid domains (exterior plus interior of all tanks). The principal modification is to impose the condition that there is no influence between the separate fluid domains. Thus the elements in the extended influence coefficient matrix are set equal to zero if the row and column correspond to different domains. Further details are given in Reference [27].

The force and moment exerted by the tank fluid on the vessel are given by

$$\mathbf{F} = \iint_{S_T} P \mathbf{N} dS = \iint_{S_T} P (\mathbf{n} + \alpha \times \mathbf{n}) dS \quad (12.63)$$

$$\mathbf{M} = \iint_{S_T} P (\mathbf{X} \times \mathbf{N}) dS = \iint_{S_T} P (\mathbf{x} + \xi + \alpha \times \mathbf{x}) \times (\mathbf{n} + \alpha \times \mathbf{n}) dS \quad (12.64)$$

where  $\mathbf{n}$  is the normal pointing out of the tank (away from the fluid domain of the tank) and double integrals are over the submerged surface of the tank.

After some vector analysis these equations give relations similar to (12.46-12.47) for the contributions from the hydrostatic pressure:

$$C_T(3, 3) = \rho g \iint_{S_T} n_3 dS$$

$$C_T(3, 4) = \rho g \iint_{S_T} y n_3 dS$$

$$\begin{aligned}
C_T(3, 5) &= -\rho g \int \int_{S_T} x n_3 dS \\
C_T(4, 4) &= \rho g \int \int_{S_T} y^2 n_3 dS - \rho g \forall_T z_c \\
C_T(4, 5) &= -\rho g \int \int_{S_T} x y n_3 dS \\
C_T(4, 6) &= \rho g \forall_T x_c \\
C_T(5, 5) &= \rho g \int \int_{S_T} x^2 n_3 dS - \rho g \forall_T z_c \\
C_T(5, 6) &= \rho g \forall_T y_c
\end{aligned}$$

All other elements of the matrix  $C_T$  are equal to zero. Here

$$\begin{aligned}
\forall_T &= \text{VOLTANK}(1) = \int \int_{S_T} x n_1 dS \\
\forall_T &= \text{VOLTANK}(2) = \int \int_{S_T} y n_2 dS \\
\forall_T &= \text{VOLTANK}(3) = \int \int_{S_T} (z - Z_T) n_3 dS \\
x_c &= \frac{1}{2\forall_T} \int \int_{S_T} x^2 n_1 dS \\
y_c &= \frac{1}{2\forall_T} \int \int_{S_T} y^2 n_2 dS \\
z_c &= \frac{1}{2\forall_T} \int \int_{S_T} (z^2 - Z_T^2) n_3 dS
\end{aligned}$$

Subroutine GEOMSTAT evaluates the hydrostatic parameters of the hull and tanks separately. Thus VOL, C(i,j) are evaluated for the hull ignoring tank patches/panels and their values are the same with or without tanks, as defined in Section 4.1. The corresponding tank parameters VOLTANK(1:3,1:NTANK) and CTANK(1:9,1:NTANK) are evaluated separately for each tank (the second index is omitted for simplicity of notation):

$$\begin{aligned}
\text{CTANK}(1) &= \int \int_{S_T} n_3 dS \\
\text{CTANK}(2) &= - \int \int_{S_T} x n_3 dS \\
\text{CTANK}(3) &= \int \int_{S_T} y n_3 dS \\
\text{CTANK}(4) &= \int \int_{S_T} x^2 n_1 dS \\
\text{CTANK}(5) &= \int \int_{S_T} y^2 n_2 dS
\end{aligned}$$

$$\text{CTANK}(6) = \int \int_{S_T} (z^2 - Z_T^2) n_3 dS$$

$$\text{CTANK}(7) = \int \int_{S_T} x^2 n_3 dS$$

$$\text{CTANK}(8) = - \int \int_{S_T} x y n_3 dS$$

$$\text{CTANK}(9) = \int \int_{S_T} y^2 n_3 dS$$

It is necessary to consider the implications of planes of symmetry with respect to the tanks. If all of the tanks are symmetric about a plane of symmetry, then it is appropriate to use that option (assuming the hull is also symmetric about the same plane). Thus, for example, for a hull with symmetry about  $y=0$ , and with all tanks symmetric about the same plane, it is appropriate to set  $\text{IS}(2)=1$ . But if there are two or more tanks along the  $x$ -axis,  $\text{IS}(1)=0$  is required. When planes of symmetry are appropriate, the following integrals (which are originally evaluated over one half or one quarter of the tank, with nonzero values), should be set equal to zero:

$$\text{If } \text{IS}(1)=1, \text{CTANK}(2) = 0, \quad \text{CTANK}(4) = 0, \quad \text{CTANK}(8) = 0$$

$$\text{If } \text{IS}(2)=1, \text{CTANK}(3) = 0, \quad \text{CTANK}(5) = 0, \quad \text{CTANK}(8) = 0$$

All other elements are multiplied by  $\text{IMUL}=2$  or  $4$  to account for the planes of symmetry, in the same manner as  $C(I,J)$ .

In GETIF, after CALL OPHEAD to output the hydrostatic matrix for the hull, the subroutine TANKFS is called when tanks are present. In TANKFS the following assignments are made for the hydrostatic restoring coefficients, where the extra terms added for the tanks are summed over all tanks associated with each body:

$$C(3, 3) = C(3, 3) + (\rho_T/\rho)\text{CTANK}(1)$$

$$C(3, 4) = C(3, 4) + (\rho_T/\rho)\text{CTANK}(3)$$

$$C(3, 5) = C(3, 5) + (\rho_T/\rho)\text{CTANK}(2)$$

$$C(4, 4) = C(4, 4) + (\rho_T/\rho) \left[ \text{CTANK}(9) - \frac{1}{2}\text{CTANK}(6) \right]$$

$$C(4, 5) = C(4, 5) + (\rho_T/\rho)\text{CTANK}(8)$$

$$C(5, 5) = C(5, 5) + (\rho_T/\rho) \left[ \text{CTANK}(7) - \frac{1}{2}\text{CTANK}(6) \right]$$

Also, if  $\text{IALTFRC}=2$ ,

$$C(4, 6) = C(4, 6) + \frac{1}{2}(\rho_T/\rho)\text{CTANK}(4)$$

$$C(5, 6) = C(5, 6) + \frac{1}{2}(\rho_T/\rho)\text{CTANK}(5)$$

The extra terms in  $C(4, 6)$  and  $C(5, 6)$  are omitted for a freely-floating body since these are balanced by the vessel's corresponding buoyancy moments.

■ When tanks are present, the header of the output file *frc.out* includes nondimensional values of the tank volumes and the contributions from the tanks to  $C(3, 3)$ ,  $C(3, 4)$  and  $C(3, 5)$ .

Next consider the inertia forces and moments due to the body mass. If IALTFRC=1 the body mass  $m$  is calculated from VOL and all of the inertia coefficients are proportional to  $m$ . Since VOL is the total displaced volume of the hull, the static mass of the fluid in the tanks is included in  $m$ . However the same inertia effects are represented (more correctly for dynamic conditions) by the added mass of the tank, to be discussed below. For this reason, if IALTFRC=1, the mass matrix BFRCOND is reduced by the sum  $\sum(\rho_T/\rho) \times \text{VOLTANK}/\text{VOLM}$ , where the sum is over all tanks. Likewise, the terms  $-mgz_g$  in the restoring coefficients  $C(4, 4)$  and  $C(5, 5)$  are reduced. If IALTFRC=2 these corrections are not made, and the external mass matrix should exclude the fluid in the tanks. If IALTFRC=1 the radii of gyration should be estimated ignoring the fluid in the tanks.

The added mass and damping coefficients are evaluated globally, by integrating the corresponding components of the pressure over both the external hull surface and the internal tank surfaces. The only modification for tank panels/patches is to multiply their contributions by RHOTANK, the relative density of the tank fluid compared to the external fluid. Since there is no radiation from the tanks, the damping coefficients should be zero. In test calculations they are generally very small, except near tank resonances. (A useful check is to verify that the damping coefficients of the hull with tanks are equal to the damping coefficients without tanks.)

Special attention is required for the vertical modes (heave, roll, pitch), where there is a fictitious hydrostatic contribution to the added mass. First consider heave, where the relevant boundary conditions are  $\phi_n = n_3$  on  $S_b$  and  $K\phi - \phi_z = 0$  on the free surface. Here  $K = \omega^2/g$ . Thus the heave potential is given by  $\phi_3 = z + 1/K$ , where  $z$  is a local vertical coordinate with its origin in the tank free surface. The heave added-mass coefficient is

$$A_{33} = \rho \int \int_{S_T} n_3 \phi_3 dS = \rho \forall_T + C_T(3, 3)/(gK) \quad (12.65)$$

Also derivable from the same potential are

$$A_{34} = \rho \int \int_{S_T} (yn_3 - zn_2) \phi_3 dS = \rho \forall_T y_c + C_T(3, 4)/(gK) \quad (12.66)$$

$$A_{35} = \rho \int \int_{S_T} (zn_1 - xn_3) \phi_3 dS = -\rho \forall_T x_c + C_T(3, 5)/(gK) \quad (12.67)$$

Since  $\omega^2 = gK$ , the last terms are cancelled by the hydrostatic restoring coefficients. Thus, in the limit  $\omega \rightarrow 0$ , there are no contributions to the equations of motion for the LHS elements associated with the vertical force or vertical translation, as expected on physical grounds.

In the classical hydrostatic analysis of ships, the tank free-surface effect is evaluated by considering the second moments of the tank free surface about a local origin at the centroid of the free surface, whereas in the expressions for  $C_T$  these moments are about the global

origin. This difference can also be explained in terms of the corresponding added mass coefficients, in an analogous manner to the analysis above.